Effects of Continuum Breakdown on Hypersonic Aerothermodynamics

Andrew J. Lofthouse[*] and Iain D. Boyd[†]
Department of Aerospace Engineering
University of Michigan, Ann Arbor, MI, 48109-2140

Michael J. Wright[‡]
Reacting Flow Environments Branch
NASA Ames Research Center, Moffett Field, CA, 94035

Hypersonic vehicles experience different flow regimes during flight due to changes in atmospheric density. Hybrid Computational Fluid Dynamics (CFD) and Direct Simulation Monte Carlo (DSMC) methods are developed to simulate the flow in different hypersonic regimes. These methods use a breakdown parameter to determine regions of the flow where the CFD physics are no longer valid. The current study investigates the effect of continuum breakdown on surface properties, such as pressure, shear stress and heat transfer rate, on a cylinder in a Mach 10 flow of argon gas for several different flow regimes, from the continuum to a rarefied gas. The difference in total drag ranges from 0.5% for a continuum to 26.2% for a rarefied gas. Peak heat transfer rate differences ranges from nearly 4% for a continuum to almost 32% for a rarefied gas. Drag depends primarily on continuum breakdown in the wake, while heat transfer rate appears to depend primarily on continuum breakdown in the shock and differences in thermal boundary layer thickness.

Nomenclature

a	=	frozen sound speed (m/s)
Kn	=	Knudsen number
L	=	characteristic length (m)
p	=	pressure (Pa)
Q	=	any flow field property such as pressure or temperature
Re	=	Reynolds number
T	=	translational temperature (K)
U	=	free stream velocity (m/s)
λ	=	mean free path (m)
μ	=	viscosity (Pa·s)
ρ	=	mass density (kg/m^3)

20060124 011

I. Introduction

A hypersonic vehicle such as a planetary entry capsule or a reusable launch vehicle, will experience vastly different flow regimes during the course of its flight trajectory because the earth's atmosphere varies in density as a function of altitude. Reproduction of these varied flow conditions in ground-based laboratory facilities is both expensive and technically challenging. Hence, there is an extremely important role for computational models in the development of hypersonic vehicles.

---

[*] Graduate Student, Member AIAA.
[†] Professor, Associate Fellow AIAA.
[‡] Senior Research Scientist, Senior Member AIAA.

The physical processes in gas dynamics can be conveniently characterized using the Reynolds number Re and the Knudsen number Kn defined as follows:

$$\mathrm{Re} = \frac{\rho U L}{\mu} \qquad Kn = \frac{\lambda}{L} \propto \frac{1}{\rho L} \qquad (1)$$

where ρ is density, U is velocity, L is a characteristic length of the flow, μ is viscosity, and λ is the mean free path. At low altitudes, the atmospheric density is relatively high, and flows around hypersonic vehicles should be simulated using traditional Computational Fluid Dynamics (CFD) by solving either the Euler or preferably the Navier-Stokes (NS) equations.[1] This is the continuum regime characterized by very large Reynolds numbers and very low Knudsen numbers. At very high altitudes, at the edge of the atmosphere, the density is very low such that there are very few collisions between the molecules and atoms in the flow around the vehicle. This is the rarefied flow regime and can be computed using the direct simulation Monte Carlo (DSMC) method.[2] Relatively speaking, CFD methods for solving the NS equations are about an order of magnitude faster than the DSMC method. However, the lack of collisions makes the physics of the NS equations invalid. The rarefied regime is characterized by a small Reynolds number and a large Knudsen number. Note that in high-Re continuum regimes, locally a flow may behave like a low-Re/high-Kn rarefied flow if the local characteristic length scale is very small. This turns out to be an important consideration as very sharp structures are being considered as an effective way to decrease drag on wing leading edges and for effective engine inlet control. Alternatively, on a blunt body, a high-density fore-body flow can create a rarefied flow in the wake of the vehicle. In principle, the DSMC method can be applied to any dilute gas flow, but becomes prohibitively expensive for Knudsen numbers less than 0.001. Thus, either CFD or DSMC on its own fails to provide a comprehensive computational modeling capability across all flow regimes encountered by a hypersonic vehicle.

A natural solution to this problem is to develop a hybrid simulation technique that employs a CFD method for as much of the flow field as possible (due to its superior numerical performance) but switch to using DSMC in regions of the flow where the physics description provided by the CFD method is inadequate. Development of such hybrid methods is an area of active research.[3,4] In this way, the CFD method would be used in the majority of the flow field while DSMC would be used in the shock and the wake regions.

A key part of any hybrid method is a reliable means to determine when to switch between CFD and DSMC within the computational domain. In general, such approaches rely on predicting incipient failure of the continuum (CFD) equations, using a so-called continuum breakdown parameter. For example, Boyd, et al[5] carried out extensive numerical investigation of one-dimensional normal shock waves and two-dimensional bow shocks comparing DSMC and CFD results to determine an appropriate breakdown parameter. They concluded that the gradient-length local (GLL) Knudsen number

$$Kn_{GLL} = \frac{\lambda}{Q}\left|\frac{dQ}{dl}\right| \qquad (2)$$

where l is some distance between two points in the flow field, and Q is some quantity of interest such as density, pressure or temperature, provides an effective indication of continuum breakdown for hypersonic compressed flows.

For design purposes it is equally important to be able to characterize the effect of a given level of continuum breakdown on design variables of interest. For hypersonic cruise or planetary entry vehicles the primary design variables are all surface quantities: heat flux, pressure and shear stress. These variables govern not only the aerodynamic performance of the vehicle, but also determine the selection and sizing of the thermal protection system (TPS), which protects the vehicle from the entry environment. However, a quantitative link between a given level of continuum-breakdown and the accuracy of predicted surface quantities using CFD has not been presented in prior studies on continuum breakdown in the literature. The goal of the present study is therefore to investigate this fundamental issue. Specifically, how are the critical hypersonic vehicle design surface properties of pressure, shear stress and heat transfer rate affected by failure of the continuum approach in certain regions of the flow field. For example, in hypersonic flow the first place where continuum breakdown is observed is within the shock wave itself. It is well known that traditional continuum CFD cannot accurately predict shock structure correctly under any circumstances.[6] It is not clear, however, whether local breakdown within the shock has a tangible impact on the rest of the flow field and the resulting surface properties.

II.   Background and Simulation Procedure

This investigation considers a Mach 10 hypersonic flow of argon over a two-dimensional, 12-inch diameter cylinder that has a fixed surface temperature of 500 K, as shown in Figure 1. The free stream density of the flow is varied such that several different regimes are considered, from the continuum through the transitional to the rarefied regime, as shown in Table 1. Knudsen numbers are calculated based on the cylinder diameter. Surface and flow field properties for this flow are presented from two different computational approaches.

First, CFD results are obtained through solution of the Navier-Stokes equations. The CFD results are obtained using the Data-Parallel Line Relaxation (DPLR) code,[7] developed at NASA Ames Research Center for the simulation of hypersonic reacting flow-fields. DPLR includes generalized models for nonequilibrium chemical kinetics, energy relaxation and surface reactions, and has been employed for the design and analysis of many Earth and planetary entry vehicles.[8,9] All DPLR solutions were generated assuming an isothermal wall at 500 K. A no-slip velocity and temperature boundary condition was enforced. In each case a grid size of 120×120 cells was employed, and the wall spacing was chosen to ensure that the cell Reynolds number ($Re_c = \rho a \Delta \eta / \mu$) at the wall was less than one everywhere on the cylinder.

Second, DSMC results are provided from the MONACO code[10] for the same flow conditions. MONACO is a general 2D/3D, parallel, unstructured mesh DSMC code that has been applied to many hypersonic, rarefied flows.[11,12] All MONACO solutions were generated using a fixed wall temperature at 500 K. Bird's variable hard sphere model was used.[2] In general, the mesh used for the final solution for each case was adapted from previous solutions such that each cell size was on the order of a mean free path. The exception was the Kn=0.002 case, where the cell size was approximately four times the mean free path and the subcell method was used to select particles for collisions.[2]

The viscosity and thermal conductivity of pure Argon in both codes were computed from collision integrals presented by Murphy and Arundell,[13] as recommended in the recent review of Wright et al.[14]
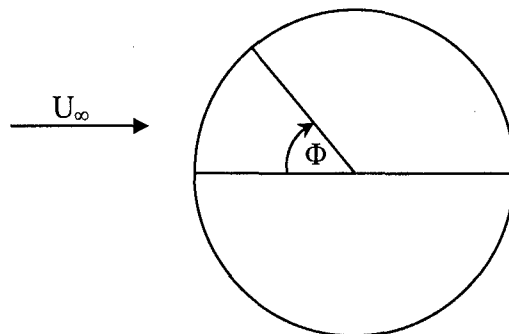

Figure 1. Geometry definition.

Table 1. Flow regimes considered.

Kn	Mass Density, kg/m³	Number Density, particles/m³
0.002	1.408×10^{-4}	2.124×10^{21}
0.01	2.818×10^{-5}	4.247×10^{20}
0.05	5.636×10^{-6}	8.494×10^{19}
0.25	1.127×10^{-6}	1.699×10^{19}

III.   Results

This investigation seeks to correlate changes in continuum breakdown of the flow around the cylinder with changes in surface properties. The overall flow features, such as temperature and density fields, are compared, as well as the surface distributions of pressure, shear stress and heat transfer. A comparison of the maximum breakdown for each case is shown in Table 2. The breakdown parameter is calculated using both the CFD and the DSMC solutions as given in Equation (2) with l being the length of a streamline in a computational cell. The CFD solution was computed using two zones, one for the fore-body area and one for the wake region (the separation point is at about $\Phi = 120°$; see Figure 1); Table 2 shows the maximum value for the breakdown parameter in each zone.

Table 2. Maximum gradient-length local Knudsen numbers, based on flow field properties according to Eq. (2), computed from CFD and DSMC solutions.

Kn	Density			Pressure			Temperature		
	CFD		DSMC	CFD		DSMC	CFD		DSMC
	Forebody	Wake		Forebody	Wake		Forebody	Wake	
0.002	0.15	0.18	0.63	0.62	0.22	0.78	0.46	0.18	0.62
0.01	0.36	0.57	0.21	1.17	0.30	0.77	1.12	0.59	0.55
0.05	0.97	35.54	0.95	1.62	57.2	1.90	1.57	31.45	1.17
0.25	6.32	1.35×10^7	38.19	2.74	1.97×10^7	53.40	5.91	1.01×10^7	19.30

Table 3. Total drag.

Kn	Drag/Length, N/m		Difference
	DSMC	CFD	
0.002	190	180	-5.19%
0.01	40.02	40.22	0.5%
0.05	8.91	9.45	6.0%
0.25	2.08	2.63	26.2%

Table 4. Peak heat transfer rate.

Kn	Peak Heating, W/m^2		Difference
	DSMC	CFD	
0.002	9.71×10^4	9.31×10^4	-4.14%
0.01	39319	40884	3.98%
0.05	16164	18191	12.54%
0.25	5984	7889	31.83%

Note that the extremely large breakdown parameter computed from the CFD solution for Kn = 0.25 is not realistic. The CFD solution predicted a density value on the lee side of the cylinder (at $\Phi = 180°$) on the order of 1×10^{-13}. Since the mean free path is proportional to the inverse of the density, this causes the mean free path to be extremely large, and hence the breakdown parameter is also extremely large. The CFD solution is not expected to be accurate in such a rarefied flow, and so these extremely high breakdown parameter values are not expected to be accurate either. Nevertheless, in a hybrid CFD-DSMC code using Kn_{GLL} as a breakdown parameter this condition would certainly flag the solver that the CFD solution is not valid in this specific region. The DSMC solutions are expected to be more realistic.

Figures 2-5 illustrate the increase in continuum breakdown, as quantified by Kn_{GLL} computed from the CFD results, as the flow becomes more rarefied. In general, the flow experiences continuum breakdown in two areas; across the bow shock and in the wake region. The flow in the shock region experiences very large gradients in flow properties, while the wake region is more rarefied, thus leading to the breakdown of the continuum hypothesis.

The maximum breakdown in the fore-body region (due to the shock) increases as the flow becomes more rarefied, although the change is not very large. In contrast, the breakdown in the wake region increases as the density drops. This increased breakdown in the wake seems to have a large effect on some of the surface properties, specifically the shear stress.

Tables 3 and 4 compare the total drag and the peak heat transfer rates predicted by both computational methods. The surface properties in each case are plotted as a function of the angle around the cylinder, with the stagnation point being located at an angle of zero (Figure 1).

A. Kn = 0.002

The current investigation only considers the flow over the fore-body of the cylinder due to the prohibitive computational expense of the DSMC method. Further investigations are planned to simulate the entire flow field around the cylinder, truncation of the domain most likely causes problems with the outflow boundary conditions, affecting the validity of the simulation. Additionally, the current DSMC simulation is not a completely converged solution, as will be discussed below.

At a Knudsen number of 0.002, this flow is well within the continuum regime. Nevertheless, there is still evidence of continuum breakdown in the shock (Figure 2), although it is only a slight amount. This small amount of

breakdown is not expected to significantly affect the surface properties. Interestingly, DSMC predicts a larger value of breakdown than does CFD (Table 2).

The temperature and density fields do not show the amount of agreement expected (Figures 6 and 7), specifically, the DSMC shock standoff distance is smaller than that for CFD. The surface pressure (Figure 8) shows very good agreement, until the point at which the DSMC domain is truncated, at which point the surface pressure drops. The DSMC shear stress (Figure 9) contains a large amount of statistical noise, indicating that more sampling iterations are required. Nevertheless, the agreement seems to be good up to the point of DSMC domain truncation, where there is a sharp increase in shear stress predicted by DSMC. The heat transfer rate (Figure 10) also shows fair agreement, but there is also some evidence of statistical noise in the DSMC results, which, unexpectedly, predicts higher heating than the CFD results. The total drag and peak heat transfer rates differ by just over 5% and 4%, respectively. This is a significant difference for a flow in which both methods are valid. The large difference in drag is most likely due to the statistical noise and the sharp increase in the shear stress. A more converged solution on a computational domain that includes the wake is expected to resolve these differences.

B. Kn = 0.01

This Knudsen number is considered to be near the limit of the continuum regime. Here there is increased evidence of continuum breakdown (Figure 3) although the maximum breakdown predicted by CFD tends to be higher than that predicted by DSMC (Table 2). In this case, the shock shows more breakdown that the wake. However, comparison of general flow field features shows that the two numerical approaches (CFD and DSMC) do not differ by a large amount. The temperature field (Figure 11) is very similar, with a few exceptions in the shock structure and the wake, where the continuum hypothesis is expected to breakdown first. The shock stand-off distance predicted by both methods is the same, as is the maximum temperature behind the shock. CFD shows a larger thermal boundary layer than DSMC. DSMC also predicts a thicker shock, as expected. The thicker shock does not seem to have an affect on the surface properties, but the smaller thermal boundary layer does seem to affect the heat transfer rate, as is shown below. Also, the minimum temperature in the wake predicted by CFD is less than that predicted by DSMC. The density field (Figure 12) is also very similar, especially in the fore-body region. The exception is the wake region, where CFD predicts an overall higher density than DSMC, as well as a pocket of higher density directly behind the cylinder than in the surrounding wake.

The amount of breakdown in the shock does not necessarily carry over to the surface properties. The surface pressure predicted by both methods is very nearly equal over the entire cylinder (Figure 13). The shear stress also shows very good comparison up to the peak value, but then DSMC predicts slightly less shear stress than CFD in the wake (Figure 14). The difference can be attributed to the more rarefied nature of the flow in this region. The total drag due to pressure and viscous effects predicted by CFD is within 0.5% of that predicted by DSMC (Table 3). The heat transfer rate shows more of a difference between CFD and DSMC along the entire surface (Figure 15). However, this difference in the present case is not very significant. The peak heating also differs by less than 4% (Table 4). This seems to indicate that the surface properties are not necessarily affected by the continuum breakdown in the shock.

C. Kn = 0.05

At a Knudsen number of 0.05, the flow is generally considered to be outside the continuum regime. Thus, the CFD results are not expected to be entirely accurate. The flow demonstrates breakdown in a larger area of the flow, primarily in the wake (Figure 4), although the CFD breakdown in the wake is much larger than the DSMC breakdown (Table 2). The differences between the CFD and DSMC temperature (Figure 16) and density fields (Figure 17) are more pronounced. The DSMC shock is much thicker than the CFD shock, although the shock stand-off distance and peak temperatures are still very nearly equal. The CFD results also show a larger thermal boundary layer than the CFD. In the wake, DSMC predicts a lower density, but a higher temperature than CFD.

The surface pressure predicted by both methods is still in excellent agreement (Figure 18). However, the shear stress is higher in the CFD results, especially in the wake (Figure 19). The point at which the CFD and DSMC shear stress results diverge is farther forward along the cylinder surface than at lower Knudsen number, and the peak shear stress is lower by about 12%. The heat transfer rate differs by an almost uniform amount along the entire surface, and difference is larger than at lower Knudsen numbers (Figure 20). The difference in total drag is still within about 6% (Table 3). On the other hand, the peak heat transfer rate differs by more than 12% (Table 4). Again, the pressure does not seem to be affected by continuum breakdown, while the shear stress seems to be affected more by the breakdown in the wake, and the heat transfer rate by the breakdown in the shock and the larger thermal boundary layer. The sensitivity of the shear stress and heat transfer to continuum breakdown is most likely due to the no-slip boundary condition imposed at the wall in the CFD method, which is invalid for higher Knudsen number flows.

D. Kn = 0.25

At a Knudsen number of 0.25, the flow is well within the rarefied regime, so large errors in flow properties are expected from the CFD method. There is more breakdown in the flow, in terms of the size of the breakdown region and the value of the breakdown parameter (Figure 5). Note that the CFD breakdown parameter in the wake is not expected to be accurate as mentioned above (Table 2). Nevertheless, the DSMC breakdown is also much larger than that for previous cases; hence the continuum hypothesis is definitely not valid in those regions. The temperature field (Figure 21) shows that the DSMC shock is much thicker, and the maximum temperature behind the shock predicted by DSMC is higher than that predicted by CFD (although the CFD heat transfer rate is still higher than the DSMC rate as discussed below). The thermal boundary layer is again larger in the CFD results than in the DSMC results. However, the shock standoff distance appears to be fairly equal. The CFD wake is much larger than the DSMC wake, and is predicted to be more rarefied, as seen in the density field (Figure 22).

The surface pressure predicted by both methods is no longer in agreement (Figure 23). At this Knudsen number, the shock has most likely merged with the boundary layer, and thus the typical shock jump relations used in the CFD method would be invalid. The DSMC pressure is less than the CFD pressure near the fore-body, but the agreement does improve in the wake. As seen in Figure 5, the breakdown in the shock region extends much closer to the surface of the cylinder and so it most likely affects the surface pressure. The shear stress shows the same general trend as in previous cases in that both methods agree near the stagnation region, but the results diverge as the flow accelerates around the cylinder (Figure 24). The DSMC shear stress is lower than the CFD shear stress, with the peak DSMC shear stress about 33% lower. The heat transfer rate also follows trends similar to the previous cases in that the DSMC heat transfer rate is lower than the CFD rate along the entire surface (Figure 25). The total drag predicted by CFD is higher than the DSMC drag by more than 26%, most likely due to the much higher CFD shear stress (Table 3). The peak heat transfer rate also differs by nearly 32% (Table 4).

IV.   Conclusion

Comparison of CFD and DSMC results for similar flow conditions show that the surface properties of pressure, shear stress and heat transfer rates are very similar for the lower Knudsen number flows, where the continuum hypothesis is valid, as expected, while for higher Knudsen number flows, while they diverge for the higher Knudsen number results. The surface pressure is least affected by continuum breakdown, as quantified by the Kn_{GLL}, among those properties investigated, and only seems to be affected by breakdown in the shock region at the highest Knudsen number flow. The shear stress is most affected by continuum breakdown and is affected primarily by continuum breakdown in the wake. This sensitivity is most likely due to the no-slip condition imposed at the wall by the CFD method, which is not valid for higher Knudsen number flows. The heat transfer rate is consistently different along the entire surface of the cylinder in all cases, although the difference increases with the more rarefied flows. This difference is most likely due to breakdown in the shock and differences in the thermal boundary layer thickness. In all cases, the surface properties predicted by DSMC tend to be lower than those predicted by CFD. As the Knudsen number increases, the difference in surface properties predicted by CFD and DSMC increases from less than 4% at Kn = 0.01 to more than 30% at Kn = 0.25.

In all cases, the CFD method was more conservative than the DSMC method, predicting a higher drag and peak heat transfer rate. In the design of planetary entry vehicles, a conservative prediction of heat transfer may not be completely undesirable in that the thermal protection shield will be designed to withstand higher temperatures than is completely necessary, but would not adversely impact vehicle performance. On the other hand, a fairly accurate prediction of drag is important since it affects the dynamics of the vehicle, and may in fact adversely affect its flight performance.

V.   Future Work

The results presented here are not comprehensive. Future investigations will explore the effect of continuum breakdown on the surface properties for an increased envelope of flow conditions. For example, flows at higher or lower Mach numbers could be investigated to determine any dependence of the correlation on flow speed. Agreement between the CFD and DSMC results can be improved by implementing a finite-slip boundary condition at the wall. Modifications to the DPLR code are being performed to implement this feature and future simulations will be compared with DSMC results. Additionally, the results presented here are two-dimensional only; three-dimensional affects will be investigated by considering the flow around an axisymmetric sphere.

Acknowledgments

References

[1] Candler, G.V., Nompelis, I., and Druguet, M.C., "Navier-Stokes Predictions of Hypersonic Double-Cone and Cylinder-Flare Flow Field," AIAA Paper 2001-1024, January 2001.

[2] Bird, G.A., Molecular *Gas Dynamics and the Direct Simulation of Gas Flows*, Oxford University Press, Oxford, 1994.

[3] Wang, W.-L., Sun, Q., and Boyd, I.D., "Assessment of a Hybrid Continuum/Particle Approach for Hypersonic Flows," *Proceedings of the 23rd International Symposium on Rarefied Gas Dynamics*, Whistler, Canada, July 2002.

[4] Schwartzentruber, T.E. and Boyd, "Detailed Analysis of a Hybrid CFD-DSMC Method for Hypersonic Non-Equilibrium Flows," AIAA Paper 2005-4829, June 2005.

[5] Boyd, I. D., Chen, G., and Candler, G. V., "Predicting Failure of the Continuum Fluid Equations in Transitional Hypersonic Flows," *Physics of Fluids*, Vol. 7, 1995, pp. 210-219.

[6] Candler, G.V., S. Nijhawan, D. Bose, and I.D. Boyd, "A Multiple Temperature Gas Dynamics Model," *Physics of Fluids*, Vol. 6, No. 11, pp. 3776-3786, Nov. 1994.

[7] Wright, M.J., Candler, G.V., and Bose, D., "Data-Parallel Line Relaxation Method for the Navier-Stokes Equations," *AIAA Journal*, Vol. 36, No. 9, 1998, pp. 1603-1609.

[8] Wright, M.J., Loomis, M., and Papadopoulos, P., "Aerothermal Analysis of the Project Fire II Afterbody Flow," *Journal of Thermophysics and Heat Transfer*, Vol. 17, No. 2, 2003, pp. 240-249.

[9] Wright, M.J., Bose, D., and Olejniczak, J., "The Impact of Flowfield-Radiation Coupling on Aeroheating for Titan Aerocapture," *Journal of Thermophysics and Heat Transfer*, Vol. 19, No. 1, 2005, pp. 17-27.

[10] Dietrich, S., and Boyd, I.D., "Scalar and Parallel Optimized Implementation of the Direct Simulation Monte Carlo Method," *Journal of Computational Physics*, 126, 1996, pp. 328-342.

[11] Boyd, I.D. and Padilla, J.F., "Simulation of Sharp Leading Edge Aeothermodynamics," AIAA Paper 2003-7062, December 2003.

[12] Sun, Q., Cai, C., Boyd, I.D., Clemmons, J.H. and Hecht, J.H., "Computational Analysis of High-Altitude Ionization Gauge Flight Measurements," *Journal of Spacecraft and Rockets,* Vol. 42, 2005.

[13] Murphy, A. B., and Arundell, C. J., "Transport Coefficients of Argon, Nitrogen, Oxygen, Argon–Nitrogen and Argon–Oxygen Plasmas," *Plasma Chemistry and Plasma Processing*, Vol. 14, No. 4, 1994, pp. 451–490.

[14] Wright, M.J., Bose, D., Palmer, G.E., and Levin, E., "Recommended Collision Integrals for Transport Property Computations I: Air Species," *AIAA Journal*, Vol. 43, No. 12, 2005, pp. 2558-2564.

[15] Gombosi, T., *Gaskinetic Theory*, Cambridge University Press, 1994.
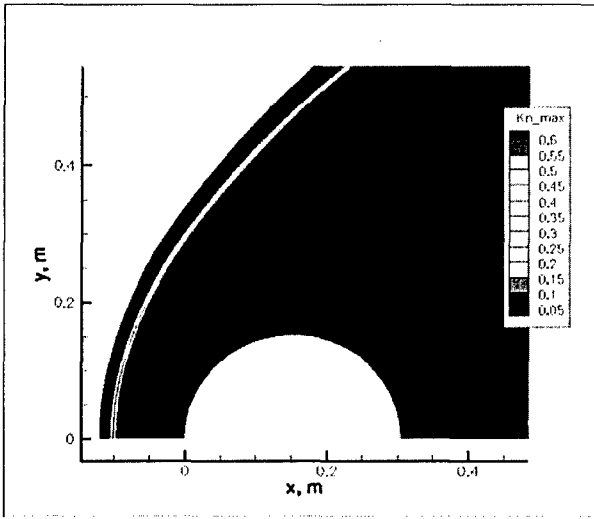
**Figure 2.** Kn = 0.002 maximum gradient length local Knudsen number.
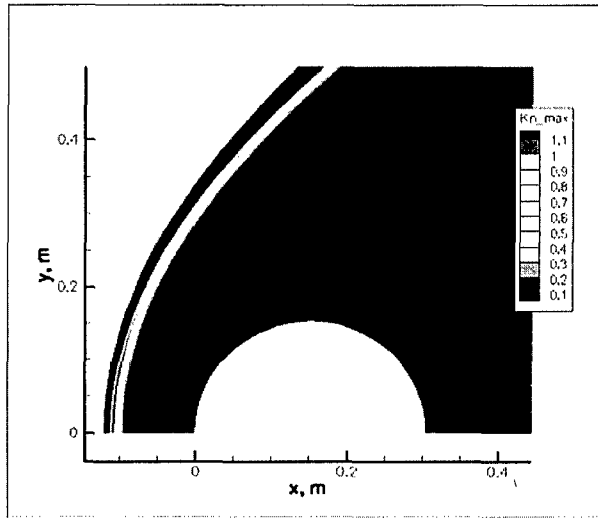
**Figure 3.** Kn = 0.01 maximum gradient length local Knudsen number.
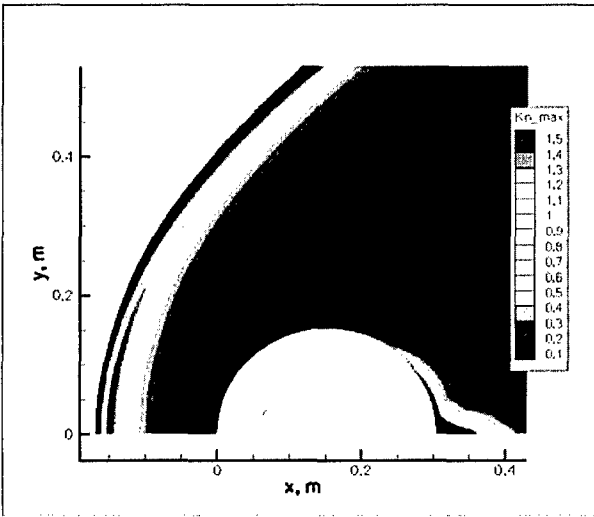
**Figure 4.** Kn = 0.05 maximum gradient length local Knudsen number.
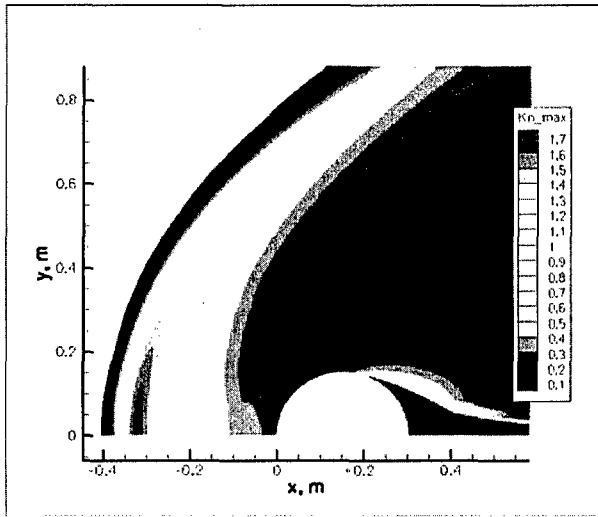
**Figure 5.** Kn = 0.25 maximum gradient length local Knudsen number.

American Institute of Aeronautics and Astronautics
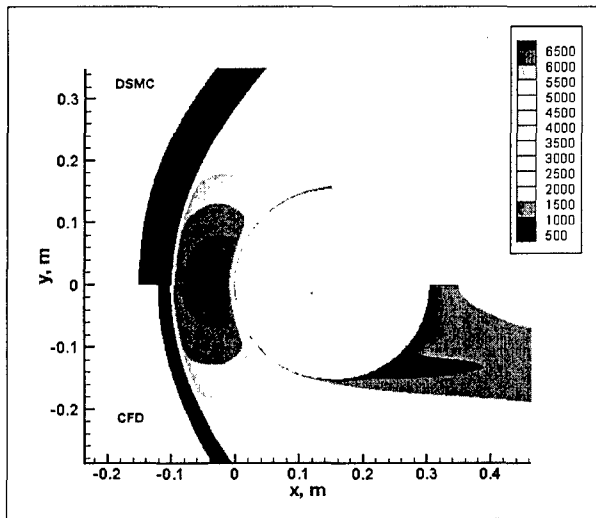
Figure 6. Kn = 0.002 Temperature field.
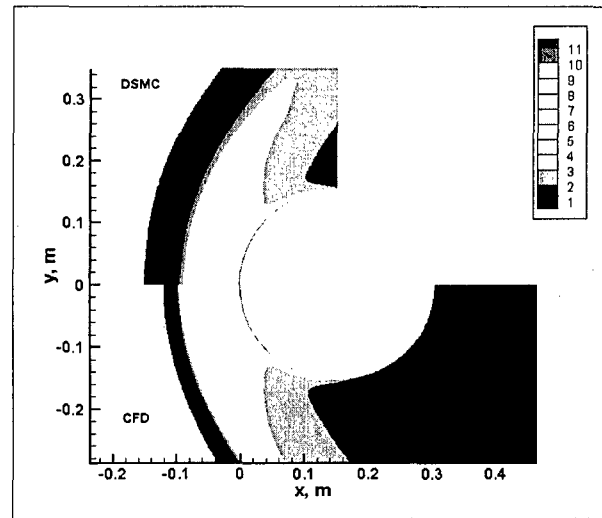
Figure 7. Kn = 0.002 Density ratio field.
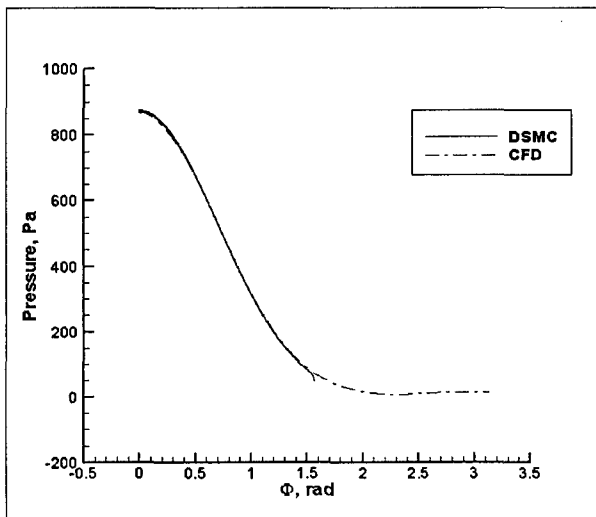
Figure 8. Kn = 0.002 surface pressure.
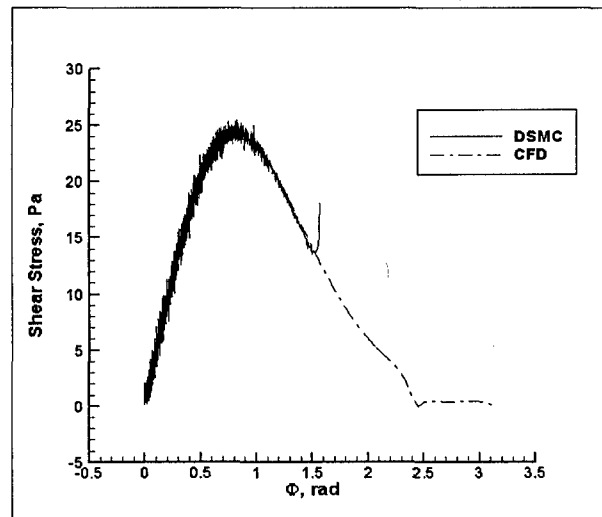
Figure 9. Kn = 0.002 surface shear stress.

9
American Institute of Aeronautics and Astronautics
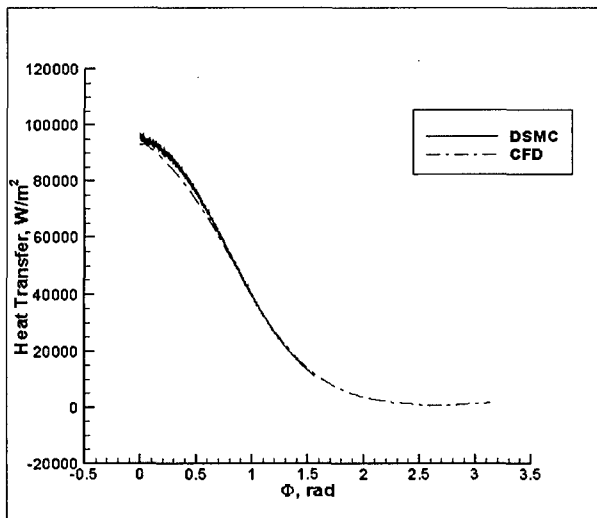
Figure 10. Kn = 0.002 surface heat transfer rate.
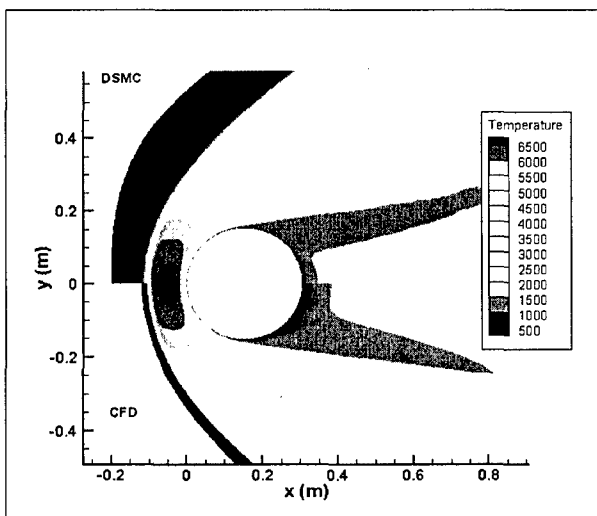
Figure 11. Kn = 0.01 temperature field.
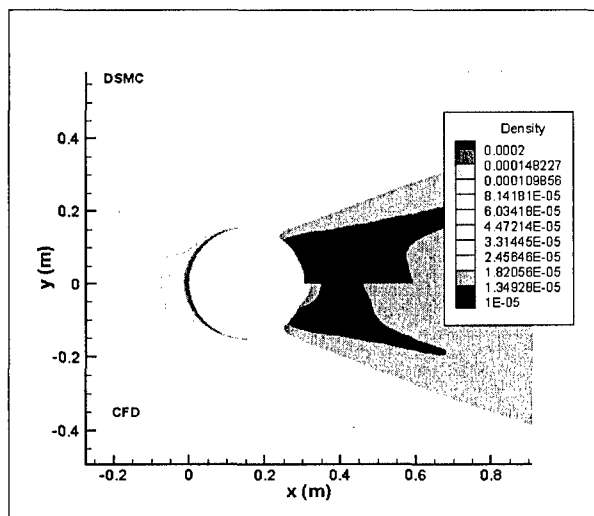
Figure 12. Kn = 0.01 density field.
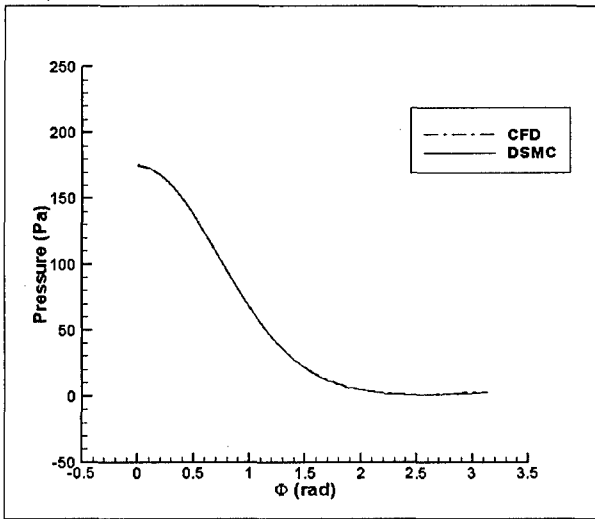
Figure 13. Kn = 0.01 surface pressure.
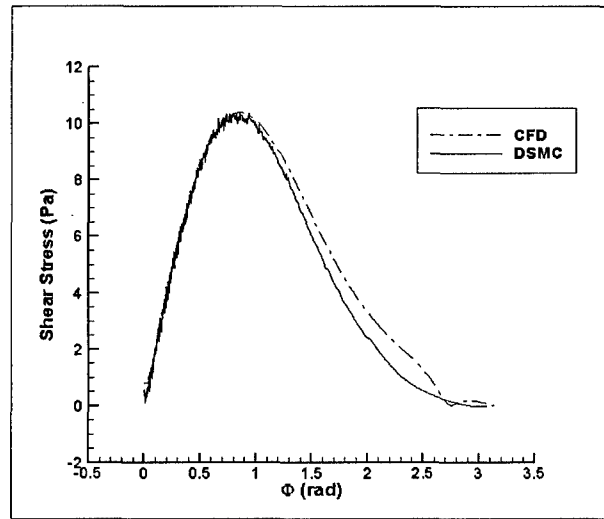

Figure 14. Kn = 0.01 surface shear stress.
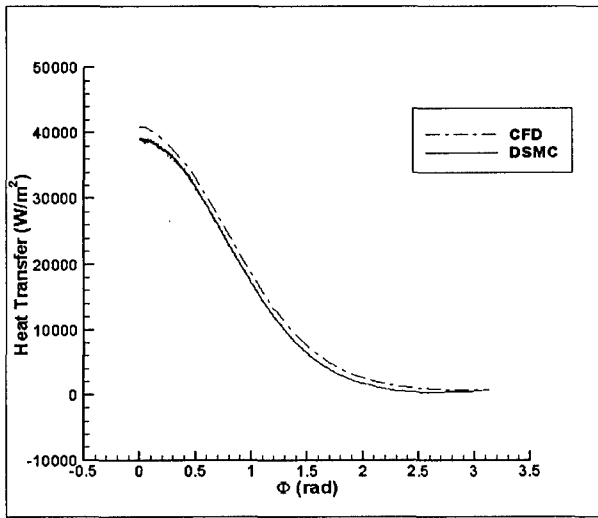
Figure 15. Kn = 0.01 surface heat transfer rate.
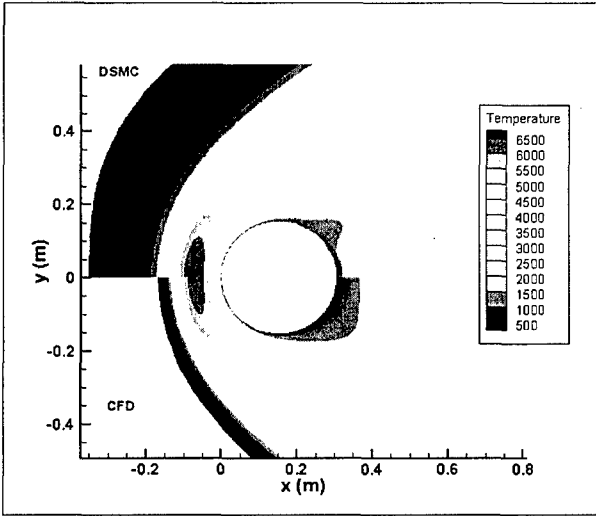
Figure 16. Kn = 0.05 temperature field.
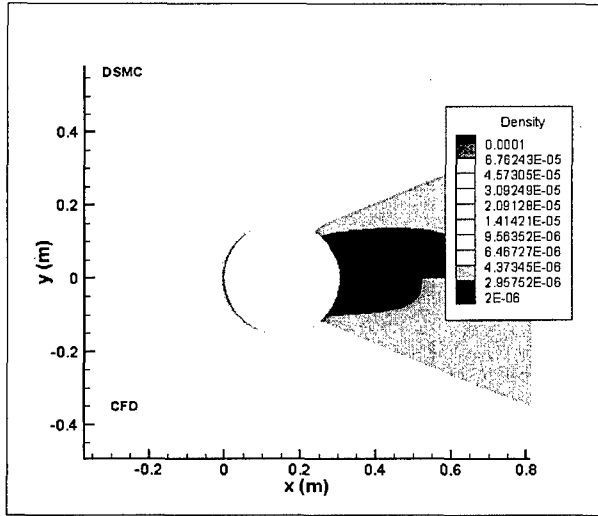
Figure 17. Kn = 0.05 density field.
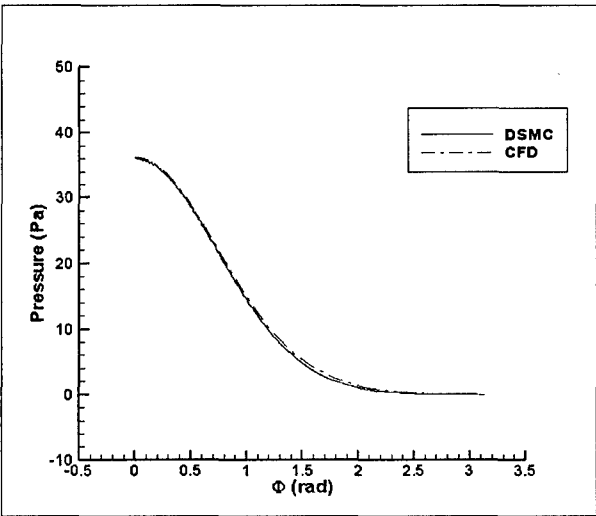
Figure 18. Kn = 0.05 surface pressure.
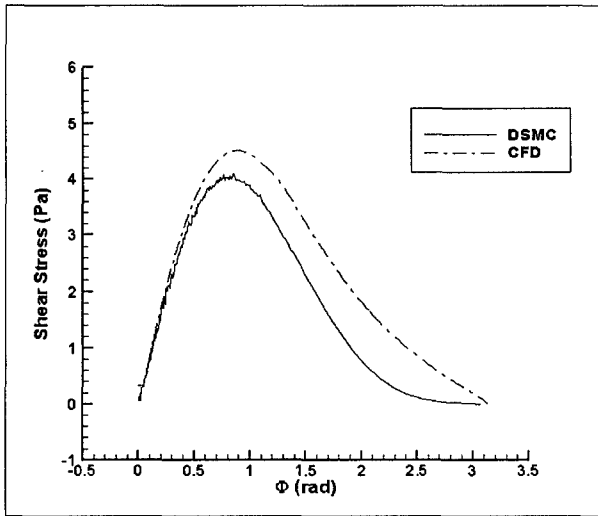
Figure 19. Kn = 0.05 surface shear stress.
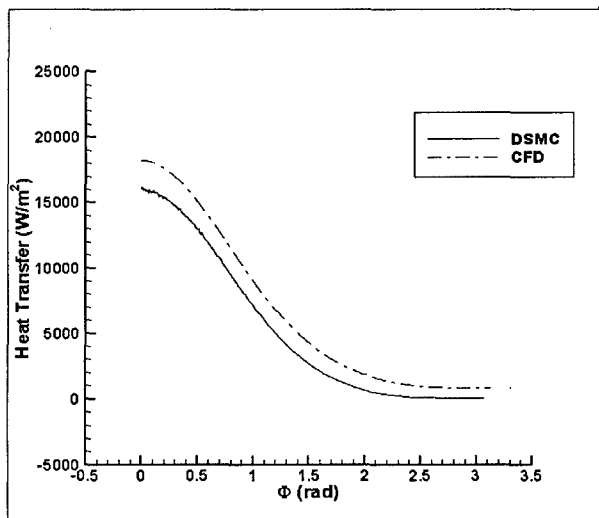
**Figure 20.** Kn = 0.05 surface heat transfer rate.
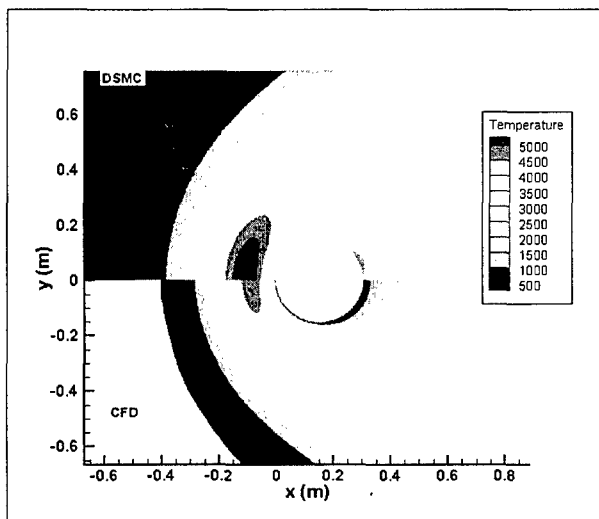
**Figure 21.** Kn = 0.25 temperature field.
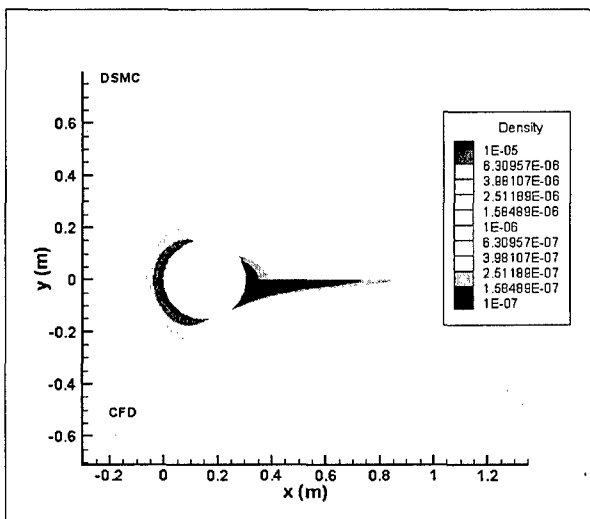

Figure 22. Kn = 0.25 density field.
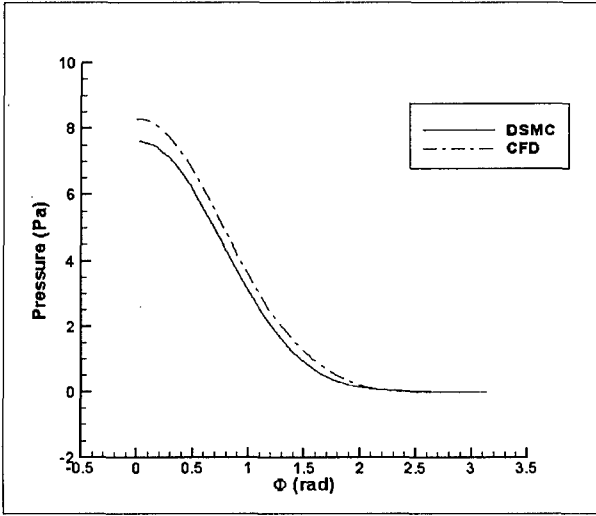
Figure 23. Kn = 0.25 surface pressure.
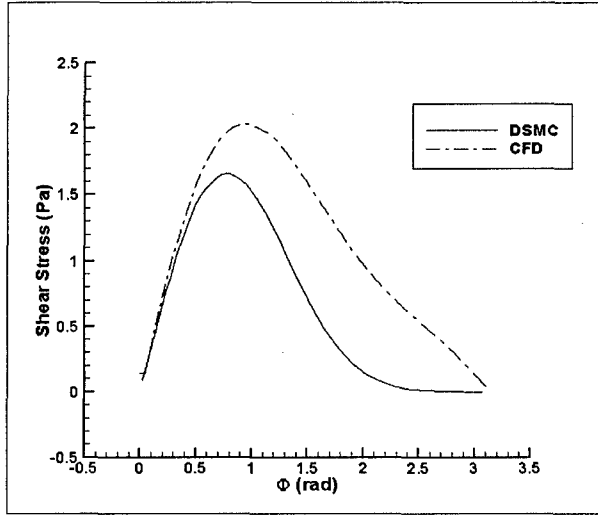
Figure 24. Kn = 0.25 surface shear stress.
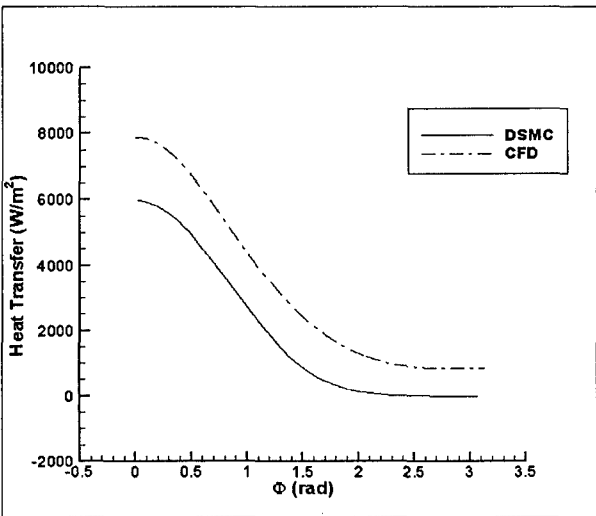
**Figure 25.** Kn = 0.25 surface heat transfer rate.

American Institute of Aeronautics and Astronautics

REPORT DOCUMENTATION PAGE		Form Approved OMB No. 0704-0188

Public reporting burden for this collection of information is estimated to average 1 hour per response, including the time for reviewing instructions, searching existing data sources, gathering and maintaining the data needed, and completing and reviewing the collection of information. Send comments regarding this burden estimate or any other aspect of this collection of information, including suggestions for reducing this burden, to Washington Headquarters Services, Directorate for Information Operations and Reports, 1215 Jefferson Davis Highway, Suite 1204, Arlington, VA 22202-4302, and to the Office of Management and Budget, Paperwork Reduction Project (0704-0188), Washington, DC 20503.

1. AGENCY USE ONLY (Leave blank)	2. REPORT DATE 9.Jan.06	3. REPORT TYPE AND DATES COVERED MAJOR REPORT

4. TITLE AND SUBTITLE
EFFECTS OF CONTINUUM BREAKDOWN ON HYPERSONIC AEROTHERMODYNAMICS.

5. FUNDING NUMBERS

6. AUTHOR(S)
CAPT LOFTHOUSE ANDREW J

7. PERFORMING ORGANIZATION NAME(S) AND ADDRESS(ES)
UNIVERSITY OF MICHIGAN

8. PERFORMING ORGANIZATION REPORT NUMBER

CI04-1723

9. SPONSORING/MONITORING AGENCY NAME(S) AND ADDRESS(ES)
THE DEPARTMENT OF THE AIR FORCE
AFIT/CIA, BLDG 125
2950 P STREET
WPAFB OH 45433

10. SPONSORING/MONITORING AGENCY REPORT NUMBER

11. SUPPLEMENTARY NOTES

12a. DISTRIBUTION AVAILABILITY STATEMENT
Unlimited distribution
In Accordance With AFI 35-205/AFIT Sup 1

12b. DISTRIBUTION CODE

13. ABSTRACT (Maximum 200 words)

DISTRIBUTION STATEMENT A
Approved for Public Release
Distribution Unlimited

14. SUBJECT TERMS	15. NUMBER OF PAGES 14
	16. PRICE CODE

17. SECURITY CLASSIFICATION OF REPORT	18. SECURITY CLASSIFICATION OF THIS PAGE	19. SECURITY CLASSIFICATION OF ABSTRACT	20. LIMITATION OF ABSTRACT

Standard Form 298 (Rev. 2-89) (EG)
Prescribed by ANSI Std. 239.18
Designed using Perform Pro, WHS/DIOR, Oct 94